Research Article Vol. 1, No. 4 / 15 Apr 2022 / Optics Continuum 826
OPTICS CONTINUUM

Single-pixel imaging with heralded single photons

STEVEN JOHNSON,[1,*] ALEX MCMILLAN,[2] CYRIL TORRE,[2,3] STEFAN FRICK,[4] JOHN RARITY,[2] AND MILES PADGETT[1]

[1]School of Physics and Astronomy, University of Glasgow, Glasgow, G12 8QQ, United Kingdom
[2]Quantum Engineering Technology Labs, H. H. Wills Physics Laboratory and Department of Electrical and Electronic Engineering, University of Bristol, BS8 1FD, United Kingdom
[3]Quantum Engineering Centre for Doctoral Training, Nanoscience and Quantum Information Centre, University of Bristol, BS8 1FD, United Kingdom
[4]Institut für Experimentalphysik, Universität Innsbruck, Technikerstraße 25, 6020 Innsbruck, Austria
[*]steven.johnson@glasgow.ac.uk
www.glasgow.ac.uk/optics/
www.bristol.ac.uk/qet-labs/

Abstract: Traditional remote sensing applications are often based on pulsed laser illumination with a narrow linewidth and characteristic repetition rate, which are not conducive to covert operation. Whatever methods are employed for covert sensing, a key requirement is for the probe light to be indistinguishable from background illumination. We present a method to perform single-pixel imaging that suppresses the effect of background light and hence improves the signal-to-noise ratio by using correlated photon-pairs produced via spontaneous parametric down conversion. One of the photons in the pair is used to illuminate the object whilst the other acts as a temporal reference, allowing the signal photons to be distinguished from background noise. Understanding the noise regime is key to producing higher contrast images using this heralding method.

1. Introduction

The ability to covertly illuminate a scene is a sought-after goal within remote sensing. For covert imaging, there is a requirement that the probe photons be indistinguishable from the fluctuations of the background light. A pulsed laser has a defined wavelength and repetition rates that allows the source to be distinguished from the background light. In contrast a source based on spontaneous parametric down conversion (SPDC) creates photons over a range of wavelengths at random times, making it a much better candidate for a covert system [1]. There have been recent developments in producing high-flux photon-pair light sources with a broad gain bandwidth that enable this covert probing of a scene to be performed [2].

Using quantum correlations to improve the signal-to-noise ratio (SNR) of imaging has been the subject of significant study [3–6] and with array sensors it has been possible to demonstrate sub-shot noise measurements using a photon-pair light source [7–9]. These correlated photons have also been utilised to distinguish signal photons from the noise photons in the background light and has been applied in a LIDAR system for range finding [10]. Indeed, a further advantage of this approach is since it is based upon random, albeit correlated, events that two or more similar systems can operate in the same environment and not suffer from cross-talk [2,11].

Here we quantify the improvement in SNR in a single-pixel imaging (SPI) system [12,13] by utilising the correlations from a photon-pair light source. SPI has been demonstrated at a variety of wavelengths [14–16], for high-speed applications [17,18], and performing depth measurements

#458248 https://doi.org/10.1364/OPTCON.458248
Journal © 2022 Received 17 Mar 2022; accepted 20 Mar 2022; published 7 Apr 2022

OPTICS CONTINUUM

[19]. In SPI a series of patterns are projected onto a target, the total power of the corresponding transmitted or back-scattered light is measured using a single-pixel detector revealing the overlap between the projected pattern and the object [20]. This method of using a single-pixel to image an unknown scene was developed alongside the field of ghost imaging, where corrected photons were used to produce images with single element detectors as a heralding system with a detector array used to identify the position of the anti-correlated photons [21], this was also shown to also be possible with classical sources [22].

During preparation of this manuscript the work by Kim et.al. [23] was published, in which a similar system is proposed for single-pixel imaging with heralded photons. In the work by Kim a rotating ground glass plate is used to increase the fluctuations found in a laser source. Within this work there is a greater focus on the magnitude of fluctuations to enable the development of systems at a range of noise sources. In addition, we use a broadband source that would be less liable to be detection above the background light sources.

In this work we demonstrate that there exists a noise regime where there is an improvement in the SNR of the images when using the photon-pair, correlated, light source. This will enable the system to be used more covertly in the presence of background light. We present a model and experimental measurements to demonstrate the operating regime for there to be an advantage via correlation measurements.

2. Measurement principle

In a classical SPI system a light source is used with an optical modulator to produce a structured illumination [24] or is used with a detector to produce a structured detection [25]. In the system presented here SPDC is used to realise a photon-pair light source. The photon-pairs are split such that one is directed to the heralding detector and the other to probe an object with a second detector behind the object, in principle this would be applicable to the back-scattered imaging arrangement but this is technologically more challenging to implement due to the high losses involved. A key parameter to achieve an advantage for the heralding measurement is to maximise the number of two-fold correlated photons. In principle the system can be used in two ways: firstly, the correlations can be ignored and the signal can be read as the total photon count from the signal detector, or secondly the correlations can be used such that the signal is read as only the counts recorded in the coincidence peak. In the first case the signal is maximised but is also subject to being confused by any background light, in the second case, the time gating means most of the background light is eliminated but at the expense of a reduced signal. It is the interplay between these two competing issues that determines the regimes in which using the source correlation might bring an advantage.

The noise in the imaging system will be proportional to the noise from a non-imaging measurement, such that we can estimate the noise in our system. The SNR of our measurement for a given integration time is given by $\mathrm{SNR} = \frac{S}{\sqrt{S+N}}$, where S is the number of counts due to signal photons and N is any additional counts arising from background noise. For the measurement where the correlations are not used (uncorrelated photons) the signal S is the total number of counts detected from the source; the noise is made up from detector dark counts N_d and the number of measured optical background counts N_b. For any real-world measurements outside of a laboratory the background levels will fluctuate due to varying frequencies of electronics and movement in the position of illumination sources, this is included as temporal changes in the background level. To emulate these temporal fluctuations a fluctuation term γ is added, where γN_b is the standard deviation in the background level with a mean value of N_b. The addition of this fluctuations will result in a larger variance than that measured from a Poissonian noise

OPTICS CONTINUUM

source. Therefore, the SNR of our uncorrelated measurement is given by

$$\mathrm{SNR}_{\mathrm{uncorr}} = \frac{S}{\sqrt{S + N_b + N_d + (\gamma N_b)^2}} \tag{1}$$

The advantage of using the correlation peak is minimising this background noise due to the gate time associated with the peak, where ε is the fraction of the noise falling within the gate time. The coincidence ratio h is the fraction of the coincidence counts divided by the total number of counts. When using the correlation peak the number of signal counts is reduced to hS. The SNR for the system to be estimated as

$$\mathrm{SNR}_{\mathrm{corr}} = \frac{hS}{\sqrt{(hS + \varepsilon(N_b + N_d) + (\varepsilon\gamma N_b)^2}} \tag{2}$$

An example of the temporal measurement of the correlated photons is shown in Fig. 1(a), with h calculated as the counts contained in the grey period divided by the total number of counts. Figure 1(b) shows the SNR calculated for a range of background and fluctuation levels for both the correlated and uncorrelated cases. For the model the values of $S = 1000$ counts, $N_d = 100$ counts, $h = 0.15$ and $\varepsilon = 0.006$ were used. When there is a higher fluctuating background light level the correlation measurement will have a higher SNR than the uncorrelated case. As Fig. 1(b) shows, the correlated measurement does not outperform the uncorrelated measurement for all possible parameters. The advantage for the correlated measurement is most apparent when the coincidence ratio h is sufficiently large relative to the inverse gate width ε. For the experimental parameters we report in this paper, we find there is no measurable advantage when using a static background signal ($\gamma = 0$) for noise levels lower than 8 times the signal level.

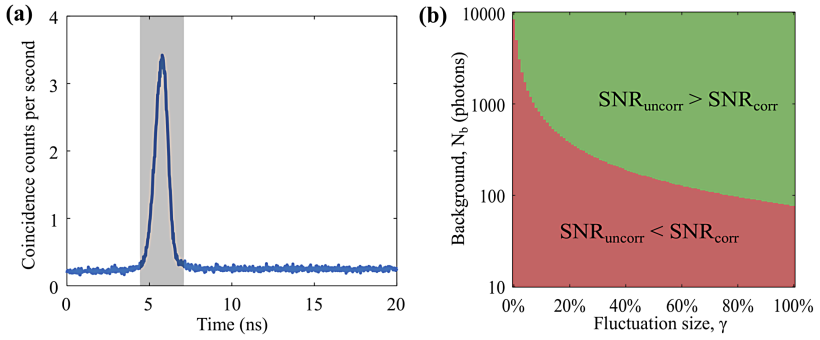

Fig. 1. (a) Time signal showing the first 20 ns of the temporal correlation measurement with our system with minimal background light present (averaged for 512 seconds). The grey area shows the region determined to be correlated photons. The counts outside of the correlation peak are from accidental photons from the source and background light. (b) A plot of the regions where there is higher SNR for the correlated and uncorrelated measurements as calculated from the model, using variables determined from our experimental system.

3. Experimental methodology

A schematic of the experimental system is shown in Fig. 2. The system comprised of a SPDC source of time-correlated photons-pairs, full details can be found in our previous work [2]. Light from a 405 nm laser diode was focused with an aspheric lens into a 30 mm long periodically poled potassium titanyl phosphate (ppKTP) non-linear crystal. The size of the crystal poling structures was linearly chirped between 9.0 µm and 13.0 µm, such that a continuous spectrum

OPTICS CONTINUUM

was produced to mimic the spectrum of background light, with both signal and idler photons spanning the range 700 nm to 950 nm. Anti-correlation in the wavelength of the pair-photons due to the energy conservation could have been used with separate wavelength bandwidth channels to improve measurement sensitivity, however this was not performed in this experiment. The pump light was removed with a long-pass filter, the orthogonal polarized signal and heralding photons are subsequently separated on a polarizing beam-splitter (PBS). These photons were focused into optical fibres to allow distribution from the system. For heralding photons, the light was focused into a multi-mode fiber (MMF) that was connected to a fiber-coupled single-photon avalanche detector (SPAD) (Excelitas Photon Counting Module SPDM CD 3416 H). For the signal photon a single-mode fiber (SMF) was used such that, after collimation with a lens, a well-defined near Gaussian beam was obtained for illuminating the object. A digital micro-mirror device (DMD), Vialux V-7001, acted as a transmission mask to pattern the light projected on to the object. The transmission object used was a three-sided star cut into cardboard. For collection of the signal photons a Horiba PPD900 photomultiplier tube (PMT) was used. The photon counting was performed with a Picoquant TimeHarp260, acting as a coincidence counter. To ensure the background light level could be controlled the DMD, target, and detector were installed within a light-tight enclosure. The background light was adjusted using a red LED (λ = 650 nm), which was connected to a National Instruments USB-6211 DAQ. The voltage on the LED was used to set the intensity level, which was calibrated from measurements from the number of photons measured by the PMT for a given voltage. As the signal measurement was not spatially resolved the measured data is largely unaffected by the exact positioning of the LED within the enclosure.

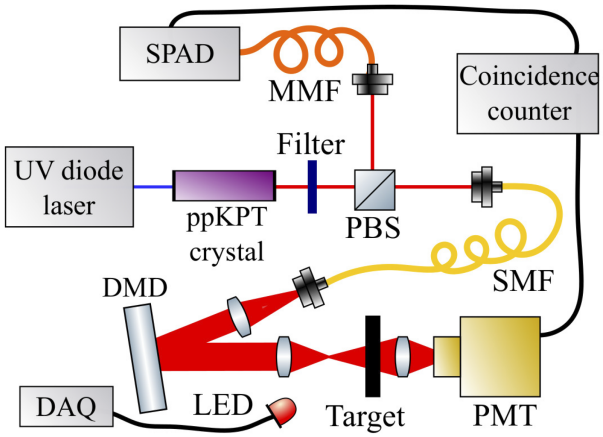

Fig. 2. The SPI experimental set up. The SPDC crystal produces 2-photons, one of which is measured by a SPAD detector as a heralding arm, the other is reflected from the DMD acting as a transparency mask, the photons transmitted through the target are recorded with a PMT. The coincidence measurement is made with a coincidence counter.

Careful alignment of the SPDC system was required to ensure a high correlation ratio, a value of 15% was achieved with the experimental system presented. For our source, the heralding photons were measured via a MMF (50 µm core diameter), the average photon level measured was 8×10^6 cps (counts per second). For illumination of the target a SMF was used (5.6 µm core diameter), which transmits 6 times fewer photons. The PMT for detection had a much lower quantum efficiency than the SPAD (1% compared to 65% for our wavelength range), there was loss due to the DMD (20% reflected) and the target was approximately 50% transparent. Therefore, the average signal after the losses was 1000 cps. Optimal collection of photons for maximising the correlation ratio will occur when SMF are used in both the signal and heralding

OPTICS CONTINUUM

arm. However, there is an increase in heralding photons if a larger optical fibre is used, but this reduces the correlation ratio.

The pattern set implemented on the DMD was the Hadamard basis [13,26], where for each pattern a measurement is made for both the positive and photographic negative patterns, the difference between these two values being the signal used in the image reconstruction. The SPI images was calculated as the differential signal for each pattern multiplied by the Hadamard matrix, the subsequent vector of the pixel values was reshaped to a square image. The Hadamard pattern size and number of illumination trials were chosen to generate a final combined output image of 16×16 pixels. With SPI compressive sensing can be used to reduce the number of measurements required [12], this would make a comparison of noise more difficult so a full sampling basis was performed for these measurements.

To produce fluctuations in the background the LED voltage was adjusted for each individual pattern measurement. The LED voltage was set to give a signal with a mean equal to the background level N_b and a standard deviation of the fluctuation level γ multiplied by N_b and a random value determined by a normal noise distribution, this value was truncated to zero for negative numbers of photons. The background light from the LED was set at the start of each measurement of a new pattern to simulate a varying photon background level. Changing at a faster rate than this would nullify the effect of the changes due to averaging. For the measurement each pattern was recorded over a 1 second acquisition for 512 patterns for a 16×16 image (8½ minutes per acquisition). The measurement was repeated for each background level and each fluctuation level between 0% and 100%. As the fluctuation level was a percentage of the background, for a zero-background level there was no background fluctuation.

For the uncorrelated case the signal was the total number of counts and for the correlated case the signal was the number of counts in the coincidence peak. To enable a comparison of the results obtained from uncorrelated or correlated measurements a ground truth image was acquired. The existing SPI system was used with a significantly higher illumination light level, a Helium-Neon laser was input into the single-mode fibre and was adjusted to give approximately 10^6 cps at the signal detector. This ground truth image of our target therefore naturally incorporated the Gaussian shape of the illumination beam that contributes to the varying intensity within the image and any image degradation due to finite resolving power of the optical system, allowing for a direct comparison of the correlated and uncorrelated strategies under the same realistic conditions of image degradation.

4. Results

SPI measurements were performed for a range of values of the background and fluctuation levels. Without background illumination an average signal level of 1000 cps was recorded for each measurement. The average number of background photons was increased from 0 up to 20 000 photons, the fluctuation size was adjusted between 0% and 100%.

The root mean squared error (RMSE) of the image reconstruction was calculated with respect to the ground truth image. The images are normalised by subtracting the mean value μ from each individual pixel and dividing by the standard deviation σ, the normalised image being defined as $x_{\text{norm}}(i,j) = (x(i,j) - \mu(x))/\sigma(x)$. The normalised reconstructed N-pixel image x is compared to the normalised ground truth image x_{gt} calculated as $\text{RMSE} = \sqrt{\sum_{n=1}^{N}(x_n - x_{\text{gt,n}})^2/N}$. Example images from the data set are presented in Fig. 3, the images are shown for a fluctuation magnitude $\gamma = 30\%$, where the background level was varied. Figure 4 presents the RMSE values for all measurements. The values of correlated ($\text{RMSE}_{\text{corr}}$) and uncorrelated ($\text{RMSE}_{\text{uncorr}}$) error measurements are compared and highlighted in Fig. 4(b). It is shown that for higher background levels there is higher RMSE in the uncorrelated measurement. It was decided that images were too noisy to identify when both RMSE>1 (an average error greater than 1 for each pixel in the

OPTICS CONTINUUM

normalised image) and neither measurement method is a valid way to acquire the image under this condition. It can be seen there are a wide range of values where the correlated measurement has an advantage over the uncorrelated measurement. There is significant agreement between our model presented in Fig. 1(b) and the measurements in Fig. 4.

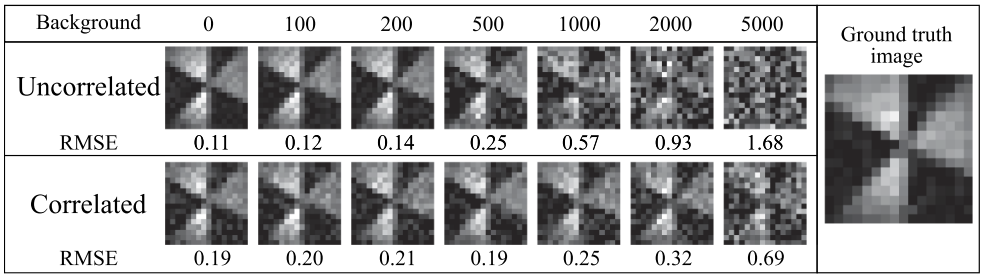

Fig. 3. An example of the images produced for both the correlated and uncorrelated measurements with the SPDC system. The data shown are for the fluctuation magnitude $\gamma = 30\%$ and varying background photon level. The root mean squared error (RMSE) calculated for each measurement is shown below each image.

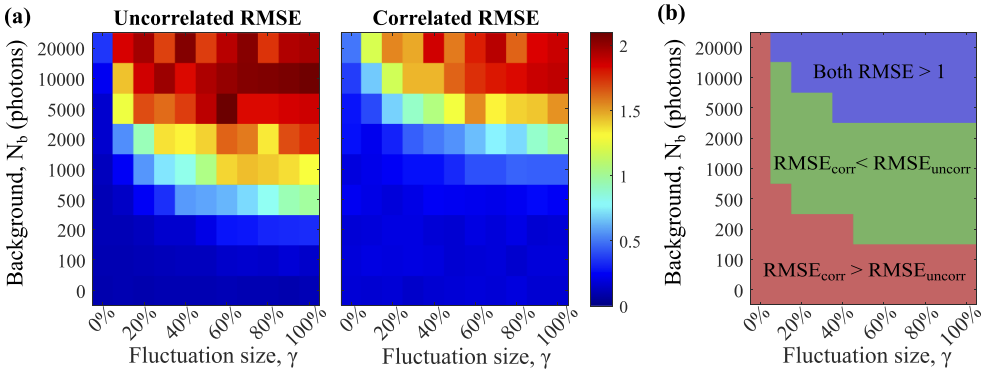

Fig. 4. (a) The RMSE calculated for the reconstructed image for the full range of measurements for varying the average photon background level and the size of fluctuation in the background during the acquisition of both the uncorrelated and correlated image. (b) A comparison of the correlated and uncorrelated images to determine under what parameters there is an advantage to using the heralding.

5. Discussion

The application of this system would be to enable sensing in a covert manner. For use outside of the laboratory there would need to be consideration of the ambient light levels and the fluctuations under these conditions. The key improvement of the temporally correlated sensing is for removal of a fluctuating background signal, the straight-forward solution to this would be to adjust the measurement time to be longer than the temporal fluctuation time of the background, thereby minimising any improvement from the correlations. A classical light source that is broadband and has random pulse timing would be feasible to be produced and would enable higher photon numbers to be used, however the SPDC system presents these characteristics in a relatively simple system. If the methodology were implemented significant improvement in the hardware would be required, if we assume a heralding rate $h = 1$ and assuming relatively small detector noise we would still require a very high photon flux from our source. For example, the source

OPTICS CONTINUUM

would need comparable output to background light; such that a photon flux 100 times lower than background could be used. As incident light levels vary with conditions an exact number of background photons is difficult to determine, however for an overcast night sky we can assumed irradiance of 10^7 photons per second per square millimetre could be considered. Therefore, for a detection with a 1 mm^2 detector a photon flux of 10^5 would be needed at detection, where losses in the projection, scattering and measurement (based on our system of 10^3 loss) would require an initial flux of 10^8, around 2 orders of magnitude greater than our current system. Another limitation will be detector saturation and electronic data transfer, both are limited to the range of 10^7 to 10^8, these would be saturated by background light with current sources without optical filtering. Suitable optical bandpass filters could be used to reduce the ambient light, but the broadband source gives the greatest advantage for covert operations, therefore there is a trade-off between removing background light and covertness. To perform this measurement in the back scattered direction we would need to consider the Lambertian scattering, with reduction in light reducing as a function of the distance to the object squared, this would produce losses of 60-100 dB for measurement in the range of metres to 1 km [27]. Whilst there may be advantage in the correlation method there are significant real-world problems that significantly reduce its effectiveness.

6. Conclusion

The model and experimental data have both shown the benefit to using a photon-pair heralding system for single-pixel imaging in the presence of background light. Introducing fluctuating background noise leads to a regime where the correlations in a photon pair source can improve the RMSE. Irrespective of using uncorrelated or correlated measurements there is a noise level where the RMSE increases to the point where it is no longer able to recover an image of the object. The limitation on the correlation measurement is down to the heralding efficiency and the maximum detectable photon rate, limited by either the photon source or detector saturation rate. However, in general heralding can give an advantage when heralding rates are not high compared to the inverse gate time. There are technological limitations due to the maximum count rate of detectors, reducing the heralding rate would increase the heralding efficiency. For remote sensing there is the significant reduction in the number of measured photons due to the huge geometrical losses associated with the collection of back-scattered light and therefore a source with a greater number of photon-pairs would be required.

Funding. Engineering and Physical Sciences Research Council (EP/S026444/1, EP/T00097X/1, EP/L015730/1).

Acknowledgments. The authors would like to acknowledge Jonathan Mathews for useful discussions.

Disclosures. The authors declare no conflicts of interest.

Data availability. Data underlying the results presented in this paper are available in [28].

References

1. J. G. Rarity, P. R. Tapster, J. G. Walker, and S. Seward, "Experimental demonstration of single photon rangefinding using parametric downconversion," Appl. Opt. **29**(19), 2939–2943 (1990).
2. S. Frick, A. McMillan, and J. Rarity, "Quantum rangefinding," Opt. Express **28**(25), 37118–37128 (2020).
3. S. Lloyd, "Enhanced sensitivity of photodetection via quantum illumination," Science **321**(5895), 1463–1465 (2008).
4. E. D. Lopaeva, I. Ruo Berchera, I. P. Degiovanni, S. Olivares, G. Brida, and M. Genovese, "Experimental realization of quantum illumination," Phys. Rev. Lett. **110**(15), 153603 (2013).
5. P.-A. Moreau, J. Sabines-Chesterking, R. Whittaker, S. K. Joshi, P. M. Birchall, A. McMillan, J. G. Rarity, and J. C. F. Matthews, "Demonstrating an absolute quantum advantage in direct absorption measurement," Sci. Rep. **7**(1), 6256 (2017).
6. T. Gregory, P.-A. Moreau, E. Toninelli, and M. J. Padgett, "Imaging through noise with quantum illumination," Sci. Adv. **6**(6), 1 (2020).
7. J. Sabines-Chesterking, R. Whittaker, S. K. Joshi, P. M. Birchall, P. A. Moreau, A. McMillan, H. V. Cable, J. L. O'Brien, J. G. Rarity, and J. C. F. Matthews, "Sub-shot-noise transmission measurement enabled by active feed-forward of heralded single photons," Phys. Rev. Appl. **8**(1), 014016 (2017).

OPTICS CONTINUUM

8. J. Sabines-Chesterking, A. R. McMillan, P. A. Moreau, S. K. Joshi, S. Knauer, E. Johnston, J. G. Rarity, and J. C. F. Matthews, "Twin-beam sub-shot-noise raster-scanning microscope," Opt. Express **27**(21), 30810–30818 (2019).
9. G. Brida, M. Genovese, and I. Ruo Berchera, "Experimental realization of sub-shot-noise quantum imaging," Nat. Photonics **4**(4), 227–230 (2010).
10. X. Ren, S. Frick, A. McMillan, S. Chen, A. Halimi, P. W. R. Connolly, S. K. Joshi, S. Mclaughlin, J. G. Rarity, J. C. F. Matthews, and G. S. Buller, "Time-of-flight depth-resolved imaging with heralded photon source illumination," in *Conference on Lasers and Electro-Optics*, (Optical Society of America, 2020), p. AM3K.6.
11. M.-C. Amann, T. M. Bosch, M. Lescure, R. A. Myllylae, and M. Rioux, "Laser ranging: a critical review of unusual techniques for distance measurement," Opt. Eng. **40**(1), 10–19 (2001).
12. M. F. Duarte, M. A. Davenport, D. Takhar, J. N. Laska, T. Sun, K. F. Kelly, and R. G. Baraniuk, "Single-pixel imaging via compressive sampling," IEEE Signal Process. Mag. **25**(2), 83–91 (2008).
13. G. M. Gibson, S. D. Johnson, and M. J. Padgett, "Single-pixel imaging 12 years on: a review," Opt. Express **28**(19), 28190–28208 (2020).
14. J. Zhang, Q. Wang, J. Dai, and W. Cai, "Demonstration of a cost-effective single-pixel UV camera for flame chemiluminescence imaging," Appl. Opt. **58**(19), 5248–5256 (2019).
15. M. P. Edgar, G. M. Gibson, R. W. Bowman, B. Sun, N. Radwell, K. J. Mitchell, S. S. Welsh, and M. J. Padgett, "Simultaneous real-time visible and infrared video with single-pixel detectors," Sci. Rep. **5**(1), 10669 (2015).
16. R. I. Stantchev, X. Yu, T. Blu, and E. Pickwell-MacPherson, "Real-time terahertz imaging with a single-pixel detector," Nat. Commun. **11**(1), 2535 (2020).
17. Z.-H. Xu, W. Chen, J. Penuelas, M. Padgett, and M.-J. Sun, "1000 fps computational ghost imaging using LED-based structured illumination," Opt. Express **26**(3), 2427–2434 (2018).
18. S. D. Johnson, D. B. Phillips, Z. Ma, S. Ramachandran, and M. J. Padgett, "A light-in-flight single-pixel camera for use in the visible and short-wave infrared," Opt. Express **27**(7), 9829–9837 (2019).
19. M.-J. Sun, M. P. Edgar, G. M. Gibson, B. Sun, N. Radwell, R. Lamb, and M. J. Padgett, "Single-pixel three-dimensional imaging with time-based depth resolution," Nat. Commun. **7**(1), 12010 (2016).
20. B. Sun, S. S. Welsh, M. P. Edgar, J. H. Shapiro, and M. J. Padgett, "Normalized ghost imaging," Opt. Express **20**(15), 16892–16901 (2012).
21. R. S. Bennink, S. J. Bentley, R. W. Boyd, and J. C. Howell, "Quantum and classical coincidence imaging," Phys. Rev. Lett. **92**(3), 033601 (2004).
22. R. S. Bennink, S. J. Bentley, and R. W. Boyd, ""Two-photon" coincidence imaging with a classical source," Phys. Rev. Lett. **89**(11), 113601 (2002).
23. J. Kim, T. Jeong, S.-Y. Lee, D. Y. Kim, D. Kim, S. Lee, Y. S. Ihn, Z. Kim, and Y. Jo, "Heralded single-pixel imaging with high loss-resistance and noise-robustness," Appl. Phys. Lett. **119**(24), 244002 (2021).
24. J. H. Shapiro, "Computational ghost imaging," Phys. Rev. A **78**(6), 061802 (2008).
25. W.-K. Yu, X.-F. Liu, X.-R. Yao, C. Wang, Y. Zhai, and G.-J. Zhai, "Complementary compressive imaging for the telescopic system," Sci. Rep. **4**(1), 5834 (2015).
26. Z. Zhang, X. Wang, G. Zheng, and J. Zhong, "Hadamard single-pixel imaging versus Fourier single-pixel imaging," Opt. Express **25**(16), 19619–19639 (2017).
27. A. McCarthy, N. J. Krichel, N. R. Gemmell, X. Ren, M. G. Tanner, S. N. Dorenbos, V. Zwiller, R. H. Hadfield, and G. S. Buller, "Kilometer-range, high resolution depth imaging via 1560 nm wavelength single-photon detection," Opt. Express **21**(7), 8904–8915 (2013).
28. S. Johnson, A. McMillan, and C. Torre, "Single-pixel imaging with heralded single photons: experimental data and analysis code," Enlighten: Research Data (2021), https://doi.org/10.5525/gla.researchdata.1215.